Obesity and Inflammation

Investigation of mechanisms of omega-3 fatty acid receptor GPR120 signaling pathway in insulin resistance and anti-inflammation and elucidation of hepatic inflammation in states of obesity

Bakk.rer.nat Ariane Pessentheiner, MSc.

University of California in San Diego

Dr. Jerrold M. Olefsky

Dr. Da Young Oh

Graz University of Technology

Dr. Juliane Bogner-Strauss

Table of contents

1. Introduction

1.1. Obesity, inflammation and insulin resistance

Obesity and its related disorders, like type II diabetes (T2D) and cardiovascular diseases, have a great importance as the number of overweight people is constantly increasing. This is not only a health related problem, but also rises up to a great economic burden[1]. The understanding of the mechanisms leading to T2D and subsequently the development of new therapeutics in the treatment of obesity and T2D are therefore of substantial need.

Obesity is a major cause for insulin resistance, which is one of the important pathophysiologies underlying the development of T2D. The reason for this relationship between excessive body fat accumulation and disturbed glucose homeostasis is considered to be obesity-related tissue inflammation[2]. Excessive nutritional fat is stored in adipocytes for periods of food deprivation, but adipose tissue (AT) is not only a storage organ, but also secretes proteins, also known as adipokines, that can have systemic effects in the regulation of glucose homeostasis and inflammation[3]. One of these mediators is tumor-necrosis factor α (TNF-α) which is secreted by adipocytes in inflammatory states and was shown to increase serum glucose concentrations[4,5].

Macrophages are important mediators of the immune system in obesity-associated inflammation. It has been shown that ATs of obese humans and rodents are infiltrated by a large number of these immune cells[6,7]. The recruitment of macrophages into adipose tissue is an initial event in obesity-induced inflammation and insulin resistance[2]. Adipocytes secrete chemokines (MCP1, LTB4), which attract monocytes from the periphery[8,9]. These monocytes migrate into the AT and become adipose tissue macrophages (ATMs). ATMs itself secrete chemokines which creates a feed forward loop in promoting inflammation.[10]

In addition to adipose tissue inflammation, chronic liver inflammation is a strong contributor to systemic insulin resistance in obesity[11]. Liver is a major site of endogenous glucose production. In normal conditions insulin stimulates the storage of glucose in the liver in form of glycogen, while endogenous glucose production is inhibited[12]. If the liver becomes insulin resistant, glucose production is enhanced and increasingly more glucose is released into the peripheral bloodstream[13]. In addition to this fact, obesity promotes fat accumulation in the liver, a morbidity which can lead to a disease called non-alcoholic fatty liver disease

(NAFLD)[14]. Similar to adipose tissue, obesity causes increased secretion of pro-inflammatory cytokines from the liver, what can attract immune cells from the periphery[11].

Studying hepatic inflammation in states of obesity is very important because inflammatory responses in the liver are very complex. Additionally, macrophages may also contribute to the development of insulin resistance in the liver[10].

Kupffer cells (KCs) are resident hepatic macrophages that become activated upon inflammation, but their number remains largely unchanged[11]. It is known that KCs are located in the hepatic sinusoidal space of Disse, where they act as phagocytotic cells which engulf

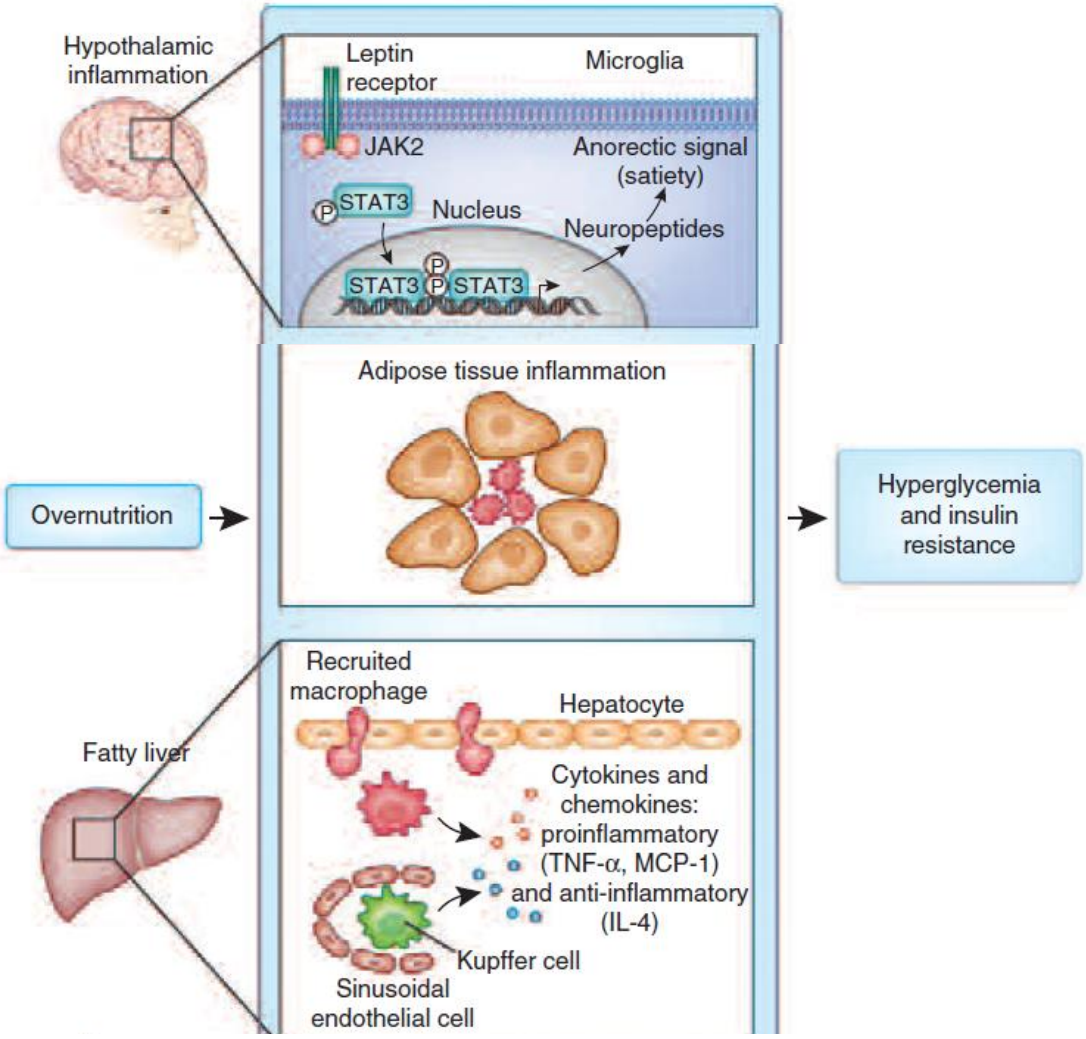

Figure 1: Contribution of brain, adipose tissue and liver to insulin resistance. Overnutrition induces inflammatory responses in these tissues which lead to systemic insulin resistance. Adapted from Osborn O. and Olefsky J.M., Nature medicine, 2012.

particles coming with the bloodstream to the liver[15]. Recently, the hypothesis arose that monocytes are recruited to the liver in states of obesity and contribute to the pro-

inflammatory machinery in obesity[16]. This hypothesis is being investigated by this study. Due to the difficulty to distinguish between Kupffer cells and recruited macrophages, a method has been established based on published methods in Dr. Olefsky's lab to discriminate those cell types[17,18]. It is important to understand the heterogeneous processes in liver inflammation for the discovery of new therapeutics in the treatment of insulin resistance in the future.

1.2. GPR120 and its anti-inflammatory properties

G protein-coupled receptors (GPCRs) play important roles in mediating various physiological stimuli into the cell. They are part of a large family of receptors, which share common structural features, such as transmembrane helices. When a ligand binds to a GPCR, it is able to activate heterotrimeric G-proteins and induces thereby cellular responses, such as modulation of cAMP production, ion channels, the phospholipase C pathway and several kinases[19].

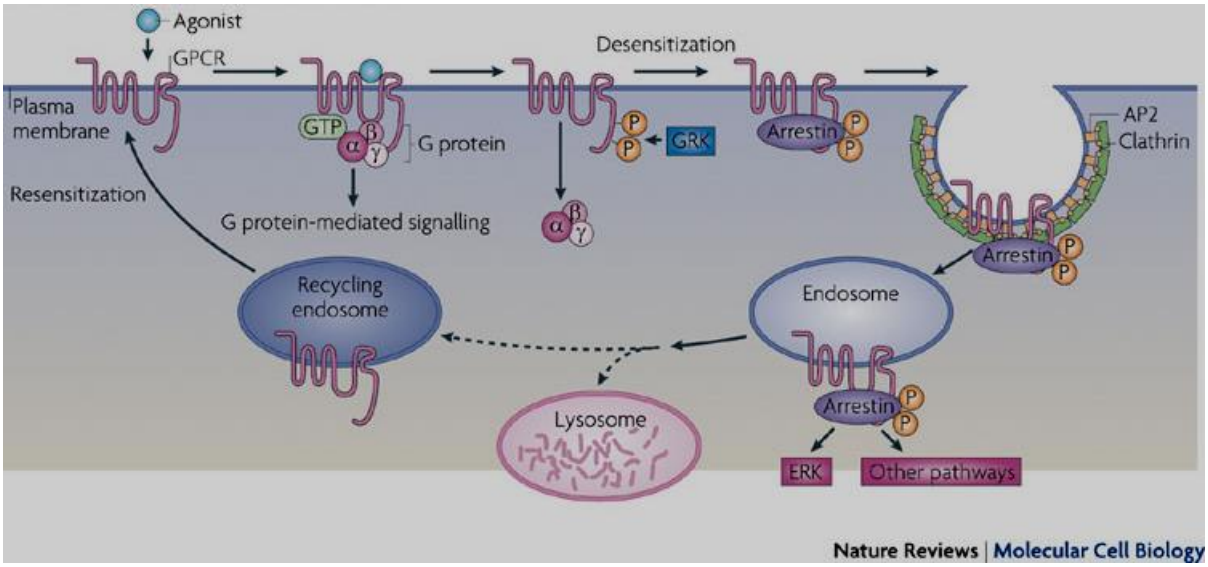

Figure 2: Scheme of Arrestin-mediated GPCR signaling. From ref. [20].

G protein-coupled receptor 120 (GPR120) is an orphan receptor which can be activated by long chain fatty acids. It is therefore also called free fatty acid receptor 4 (FFAR4)[21]. Oh et al. discovered that GPR120 is highly expressed in adipose tissue and in pro-inflammatory macrophages[22]. Furthermore, they showed that GPR120 plays an important role in the regulation of inflammatory responses. Natural ligands of this receptor are omega-3 fatty acids (ω-3 FAs), such as docosahexaenoic acid (C22:6n3; DHA), which is a major

component of fish oil. When GPR120 gets activated by a synthetic agonist or DHA, it exerts potent anti-inflammatory and insulin-sensitizing effects[22].

GPR120 has been shown to interact with β-arrestin2, which is a crucial binding partner for the action of GPR120[22]. B-arrestins are adaptor proteins which associate with the intracellular domain of GPCRs after they are stimulated by their ligands. This couples the receptor to specific downstream mechanisms, terminates their signal transduction or mediates receptor endocytosis[23,24]. A scheme of this action can be seen in figure 2.

In addition to its role in inflammation, GPR120 was also reported to be involved in the differentiation of preadipocytes into adipocytes[25]. Silencing of GPR120 *in vitro* in adipogenic cells inhibited differentiation[25], but a total-body knock-out of GPR120 increased obesity in mice on HFD ,and inhibited activity of GPR120 correlates with obesity in humans[26]. Adipogenesis is a process regulated by many genes, of which PPARγ is the so-called master regulator[27]. Many genes are reported to be PPARγ target genes, amongst them genes I am working on such as adipocyte plasma membrane associated protein (Apmap)[28] and α/β-hydrolase domain containing protein 15 (Abhd15)[29].

There are several indications that GPR120 is also regulated by PPARγ (all from [25]):

-) Its expression is upregulated during differentiation of adipocytes.
-) Expression pattern resembles PPARγ expression.
-) The PPARγ agonist troglitazone increases the expression of GPR120.

Based on these results and unpublished observations, we wanted to investigate the functional binding of PPARγ to the GPR120 promoter region. To narrow down possible interaction sites, we explored already published datasets, in which the global binding of PPARγ was investigated [30–32]. Due to these results, we identified 5 possible interaction sites within the GPR120 promoter and inserted them into luciferase reporter vectors for testing functional PPARγ binding.

Obesity-associated inflammatory changes leading to insulin resistance have been also described in the central nervous system (CNS), including the hypothalamus[33]. The hypothalamus controls energy homeostasis in the whole body and plays therefore a central role in the development of insulin resistance[33]. Microglia are resident macrophages in the CNS that can be activated and are able to perform phagocytosis and release various cytokines[34]. It has already been shown that DHA may have neuroprotective effects after brain injury, but exact mechanisms how DHA evokes its positive effects are unknown[35].Other beneficial effects of unsaturated fatty acids on hypothalamic inflammation in diet induced

obesity have been shown by Cintra et al.[36]. In this publication it was also shown that GPR120 is expressed in the hypothalamus. To investigate the role of GPR120 in brain more detail, this part of the project aims to isolate microglia from adult mouse brains and the investigation of the expression of GPR120 in these cells.

Taken together, GPCRs in general are important targets for the development of new therapeutic agents and especially the investigation of the role GPR120 in inflammation and glucose homeostasis harbors promising tools in the fight of obesity and associated diseases such as insulin resistance[37].

2. Aims

a) Application of methods to distinguish resident and recruited liver macrophages and investigation of their genetic profile.
   In order to distinguish between resident liver macrophages and recruited monocytes a method has been developed and improved which is based on the differential labeling of differently derived immune-cells and thereafter the analysis of this populations with flow cytometry (FACS).
b) Investigation of the role of PPARγ in the regulation of GPR120 gene expression and the potential PPARγ binding sites within the GPR120 promoter.
c) Investigation of the dependency of GPR120 expression in different tissues on feeding various diets (HFD, FOD, synthetic GPR120 agonist-diet) and isolation of microglia of lean and obese mice and investigation of GPR120 expression in these cells.

3. Materials and Methods

Animal care and use

Male C57Bl/6 mice were fed a normal chow (13.5% fat; LabDiet) or high-fat diet (HFD; 60% fat; Research Diet) *ad libitum* for 15-20 weeks from 8 weeks of age. Mice were switched to fish oil diet (FOD, an isocaloric HFD-containing 27% EPAX oil replacement (wt/wt; EPAX oil: 10% EPA (C20:5n3), 40%, DHA (C22:6n3), Research Diet)) or a HFD supplemented with the synthetic GPR120 agonist, compound A (30 mg/kg) after 15 weeks of HFD and were kept for further 5 weeks on this diet. Animals were housed in a specific pathogen-free facility and given free access to food and water. All procedures were approved by the University of California San Diego animal care and use committee.

Monocyte preparation

Leukocyte pools from C57BL/6 male mice 12 weeks of age, bled by retro orbital sinus, were subjected to red blood cell lysis and monocyte subsets were enriched with EasySep® mouse monocytes enrichment kit (STEMCELL tech, Vancouver, BC) followed by manufactures' instruction.

In vitro labeling

Isolated monocytes ($5x10^6$ to $10x10^6$) were washed once in serum-free medium (RPMI-1640) and suspended in 2 ml of Diluent solution C (included in the PKH26 labeling kit). Two ml of PKH26 (Sigma Chemical Co. St Louis, MO) at $2x10^{-3}$ M in Diluent C was added and mixed, and the cells were incubated for 10 min at room temperature in the dark. The staining reaction was stopped by addition of an equal volume (2 ml) of medium supplemented with 10% FBS. The mixture was centrifuged and the cells were washed once and resuspended in serum containing medium and counted.

In vivo migration

Subsequent to labeling with PKH26, the monocytes were counted and ~$1x10^6$ viable cells were suspended in 0.2 ml PBS and injected into the retro orbital sinus vein of each group of

mice. Two days after injection, the adipose tissue macrophages (ATMs) and liver non-parenchymal cells were isolated and analyzed by FACS.

Isolation of bone marrow cells for reconstitution

Bone marrow was flushed out of the fibular and femoral bone of C57BL/6 mice and washed 3x with ice cold PBS. Then the cells were passed through a syringe to avoid clots. After a red blood cell lysis was performed, the cells were counted and resuspended in serum containing RPMI Medium.

Kupffer cell labeling model

8-week old C57/B6 mice were injected i.v. with green polychromatic latex beads (Fluoresbrite 0.5 um, Polysciences Inc.). Two days after the injection the mice were irradiated with a dose of 10 Gy and 6 hours after irradiation the mice were reconstituted with $1.5x10^6$ bone marrow cells isolated C57BL/6. Two weeks after reconstitution non-parenchymal cells were isolated from the liver and white adipose tissue.

Liver non-parenchymal cells isolation (Kupffer cells and recruited macrophages)

Non-parenchymal cells (NPC) were isolated from the liver as described before[18]. Because adaptations to protocol were made in the procedure, the whole method is described below. The cells were sorted with a BD Biosciences FACS Aria III cell sorter to isolate FITC and PKH single positive cells and plated on 24 well culture plates over night or were pelleted (1000g, 10 min) and immediately used for RNA isolation. FITC and PKH positive cells were then stimulated with 10ng/ml LPS for 2 hours. The expression of inflammatory genes was assessed by qPCR.

All buffers were supplemented with DNaseI (0,02 mg/ml, Roche). The liver of anesthetized mice (ketamine 25 mg/kg, xylazine 2 mg/kg, acepromine 1 mg/kg) was perfused with SC1 buffer (8 g/L NaCl; 0,4 g/L KCl; 0,078 g/L NaH_2PO_4 x H_2O; 0,12 g/L Na_2HPO_4; 2,38 g/L HEPES; 0,35 g/L $NaHCO_3$; 0,19 g/L EGTA; 0,9 g/L glucose; pH 7,4) via the portal vein for 2-3 min to wash the liver, followed by perfusion with 50 ml SC2 (SC1 plus 0,56 g/L $CaCl_2$ x $2H_2O$) buffer containing collagenase D (0,36 mg/ml, Roche) (10 ml/min infusion speed) for *in situ* digestion. Immediately after perfusion, the liver was removed and minced with scissors. After adding 30 ml SC2 containing 0.07 mg/ml pronase E (Merck, EMD), the specimens were incubated for 20 min at 37 °C with permanent stirring. The liver specimen was filtered

through a 100 µm nylon-cellstrainer, suspended in SC2 and centrifuged 5 min at 50g at room temperature to remove hepatocytes. This step was repeated 3 to 4 times and non-parenchymal cell-enriched supernatants were kept. After removing hepatocytes, the non-parenchymal cells were pelleted at 600g for 5min at 4°C and thereafter purified using centrifugation with Percoll-GBSS Solution (Gey' balanced salt solution, 36% Percoll) at 800g 20 min, 4°C in a swing-out rotor without brakes. The pellet was washed ones with GBSS. After red blood cell lysing, the cells were washed twice and subjected to flow cytometry or stained with antibodies prior to FACS analysis.

Fluorescence-activated Cell Sorting (FACS) analysis of liver macrophages

For liver macrophage analysis, Kupffer cells were prepared by two-step liver collagenase digestion and fractionation on a density gradient as described above. The antibodies for surface staining were F4/80 (BM8) and CD11b (M1/70) (eBioscience, San Diego, CA).
Liver NPCs were sorted with a BD Biosciences FACS Aria III cell sorter to isolate FITC and PKH single positive cells and plated on 24 well culture plates overnight.

RNA isolation and quantitative-PCR

Total RNA isolation was performed with TRIzol reagent (Life Technologies, Carlsbad, CA) according to the manufacturer's instructions. For cDNA synthesis GoScript reverse transcription system was used (Promega, Madison, WI) and quantitative PCR (q-PCR) was performed as described previously[38]. Gene expression levels were calculated after normalization to the standard housekeeping gene *RPS3* and *GAPDH* using the $\Delta\Delta C_T$ method[38], and expressed as relative mRNA levels compared with internal control. Primer information is available upon request.

Promoter analysis

Four putative PPARγ binding regions upstream from the transcription start site of GPR120 and one region in intron 1 have been selected regarding to ChIP sequencing results[30,31] (see figure 6 for corresponding regions). These regions (referred to as peak intron, and peak 1-4) have been cloned into pGL4.26 (Promega) or pTK-Luc (Addgene plasmid 1015) reporter vectors, respectively. Due to a highly GC rich region in peak 1, this peak has been separated into 2 shorter sub-peaks.

Luciferase reporter assay

HEK293 and Cos7 cells were maintained in DMEM (4,5g/L glucose) supplemented with 10% FBS and cultivated at 37°C in 10% CO_2.

For reporter assay, Cos7 or HEK293 cells were cotransfected with pCMX_RXRα, pCMX_PPARγ2 (kind gift of E. Rosen) and either mouse GPR120 promoter constructs in pTKLuc reporter vector or an empty vector as control. PPRE 3x-TK-Luc (Addgene, Cambridge, MA) was used as a positive control. Transfections were performed with SuperFect (QUIAGEN, Valencia, CA) in 24-well plates according to manufacturer's instructions. Twenty-four hours after transfection, cells were treated with 10 µM rosiglitazone (Sigma Aldrich, St. Louis, MO) for 24 hours. Thereafter, cells were harvested, and luciferase activities in the cell extracts were measured with luciferase assay system (Promega) for firefly luciferase and Renilla-Glo luciferase system (Promega) in a luminometer (Berthold). Firefly luciferase values were normalized to *Renilla* luciferase vector pGL4.75.

Microglia isolation

Isolation of mouse microglia was performed as a combination of the method provided by Cardona *et al*.[39] and a commercial available kit using antibody magnetic beads for selection (CD11b Microbeads with the MACs system, Miltenyi Biotec, Bergisch Gladbach, Germany).

Briefly, the brain of mice on NC, HFD or FOD was dissected, washed in ice-cold PBS, minced and incubated gently rocking in 10ml digestion buffer (HBSS supplemented with 0.05% collagenase D, 0.1µg ml^{-1} TLCK, 0.025 Uml^{-1} DnaseI and Rnase inhibitor) for 15 min at room temperature. After that, cells were filtered through a 100 µm nylon cell-strainer and were centrifugated for 7 min at 300g. Cells were washed once with HBSS and then the cellsuspension was further used for microglia isolation according to the recommendations of the Microbeads kit's protocol. All volumes have been upscaled according to the cell number.

Data analysis

The values presented are expressed as the means±SEM. The statistical significance of the differences between various treatments was determined with the student's t-test. $p<0.05$ was considered significant.

4. Results

4.1. Isolation and characterization of resident and recruited liver macrophages in lean and obese C57BL/6 mice

Previous results obtained in Dr. Oh's and Dr. Olefsky's lab showed that obese mice have an increased population of liver macrophages that cannot be found in lean animals (fig. 4). This population is referred to as R3 in figure 4. The cells in this population are smaller and less granular than R2 cells when comparing the side scatter and forward scatter in figure 3 (red… R3 cells, green… R2 cells). These results led to the hypothesis that the population found in R3 is comprised by newly recruited monocytes that come to the liver in states of obesity.

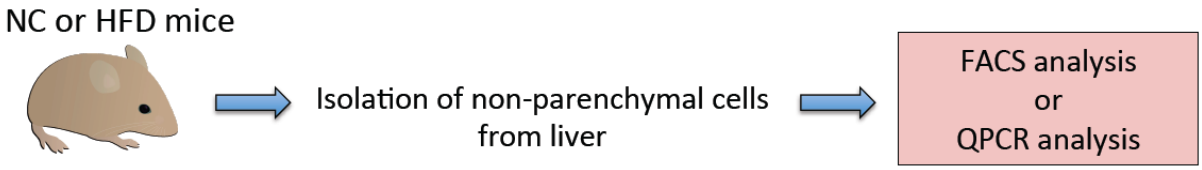

Figure 3: Typical workflow of liver macrophage isolation and analysis.

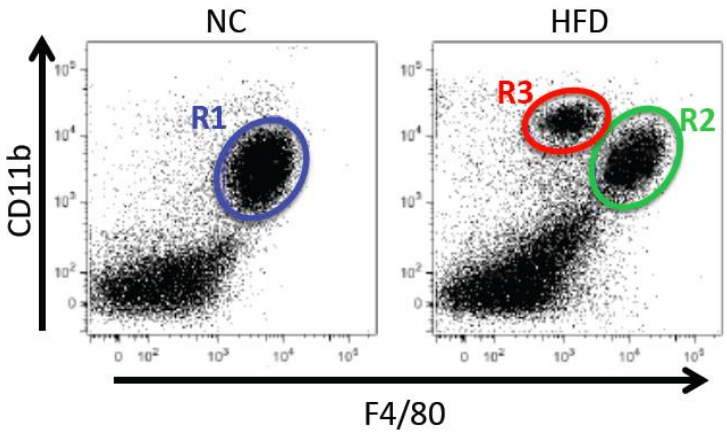

Figure 4: Hepatic non-parenchymal cells of normal chow (NC) and HFD mice. Cells were surface labeled with CD11b and F4/80 and analyzed regarding their surface label with FACS.

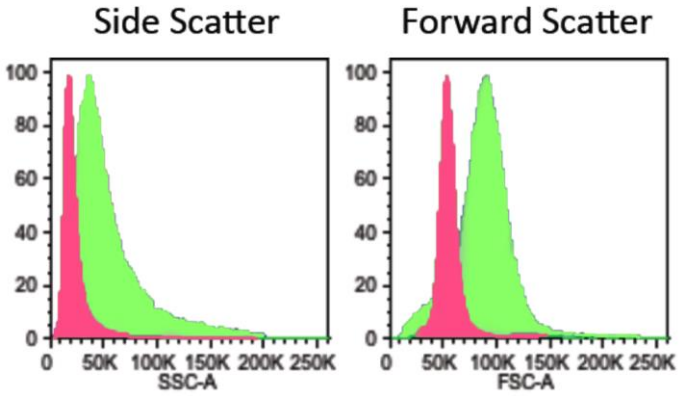

Figure 5: Side-scatter (SSC-A) and forward-scatter (FSC-A) analysis of hepatic non-parenchymal cells of R2 (green) and R3 (red) populations from figure 3.

We used a method previously established in Dr. Olefky's lab by Oh et al.[17] and changed the protocol to address this hypothesis. In this method FITC labeled latex beads were injected into normal chow (NC) and HFD mice before mice underwent a lethal irradiation. All phagocytic cells, such as macrophages, take up these beads and become labeled. After the irradiation, mice were reconstituted with bone marrow of wild type (WT) mice. Kupffer cells (KCs) are relatively resistant to irradiation and the only immune cells in the liver that survive this lethal dose[40]. After recovery, the mice are injected monocytes labeled with the fluorescent dye PKH26. After isolation of non-parenchymal cells from the liver, the cell populations can now be distinguished between resident KCs (green fluorescent label) and newly recruited hepatic macrophages (RHMs) from the periphery (red fluorescent label). The cells were separated, counted and sorted regarding their fluorescent label with flow cytometry. The cells were also plated, cultured and used for further investigation, e.g. analysis of genetic profiles with qRT-PCR and measurement of inflammatory markers, such as TNF-α release. The whole method is summarized in fig. 6.

Fig. 7 clearly shows that the number of resident KCs did not change upon high fat feeding of mice, but RHMs are 6-fold increased in obese animals. We also observed a small population of FITC and PKH26 double positive cells which most likely represent macrophages that had engulfed free latex beads or phagocytozed dying bead positive cells.

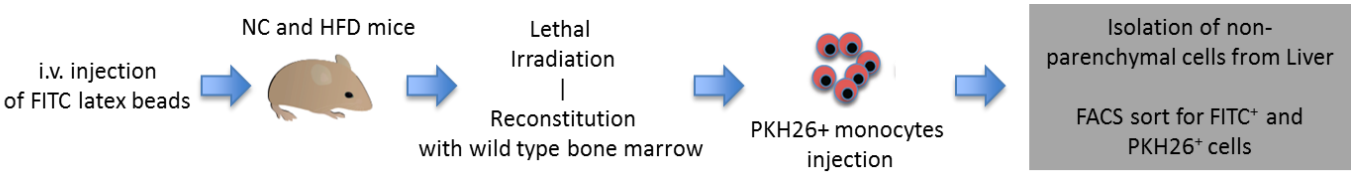

Figure 6: Workflow used to discriminate between resident Kupffer cells and newly recruited liver macrophages.

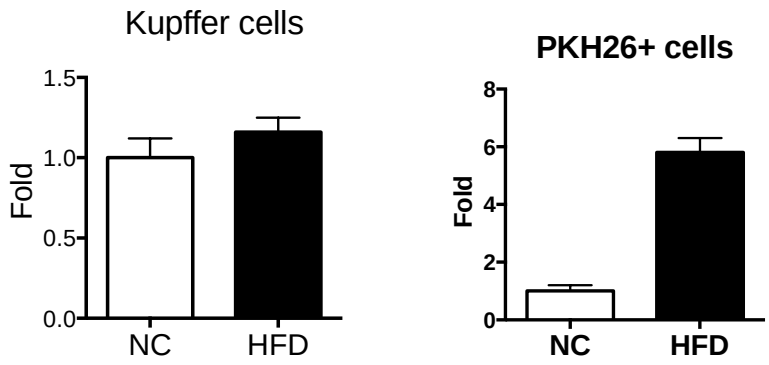

Figure 7: Relative number of Kupffer cells vs. PKH26 positive cells in normal chow (NC) and HFD mice.

Next, we analyzed PKH26+ recruited hepatic macrophages and FITC+ Kupffer cells in a dot plot with forward scatter on the Y and side scatter on the X axis. Figure 8 shows that RHMs are significantly smaller in size while KCs were larger and more heterogeneous in size, consistent with Figure 5.

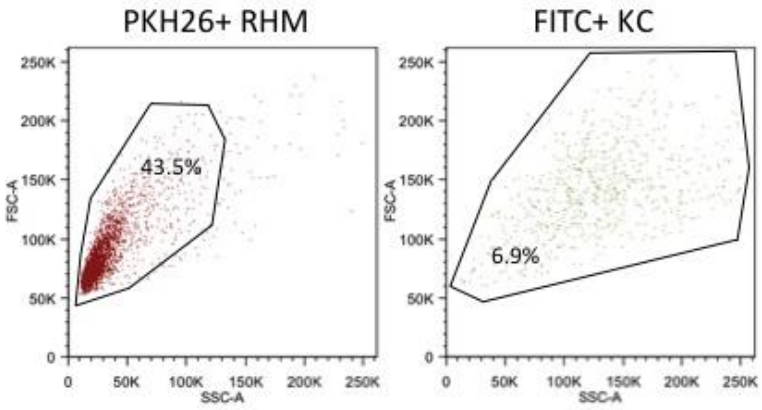

Figure 8: Side-scatter (SSC-A) and forward-scatter (FSC-A) analysis of hepatic non-parenchymal cells of PKH26+ recruited hepatic macrophages (RHM; left panel) and FITC+ Kupffer cells (KCs; right panel) after sorting.

4.2. Investigation of putative PPARγ binding sites in the promoter region of GPR120

After analysis of ChIP sequencing data of 2 different groups, 4 regions upstream of the transcription start site (TSS) of GPR120 and one region within intron 1 were selected for testing a putative PPARγ binding according to their result to show a PPARγ binding peak in mouse adipocytes, epididymal WAT (eWAT) or inguinal WAT (iWAT) (figure 9). These regions were cloned into firefly-luciferase vectors and co-transfected with PPARγ and its heterodimeric binding partner RXRα. After that, cells were stimulated with the PPARγ agonist rosiglitazone for 24 hours and the luciferase activity was measured after that time. A reporter vector containing three copies of the PPARγ response element (PPRE)[41] was used as positive control in all assays. As seen in figure 10 and 11 none of the construct showed enhanced luciferase activity, although some of the constructs exhibited a very high basal activity when cloned into the pGL4.26 reporter vector. This may due to the minimal promoter present in the vector pGL4.26, therefore we also analyzed the constructs in a different vector, namely pTK-Luc that only contains the luciferase reporter gene to an upstream thymidine kinase promoter. This vector was modified from PPRE X3-TK-luc[42].

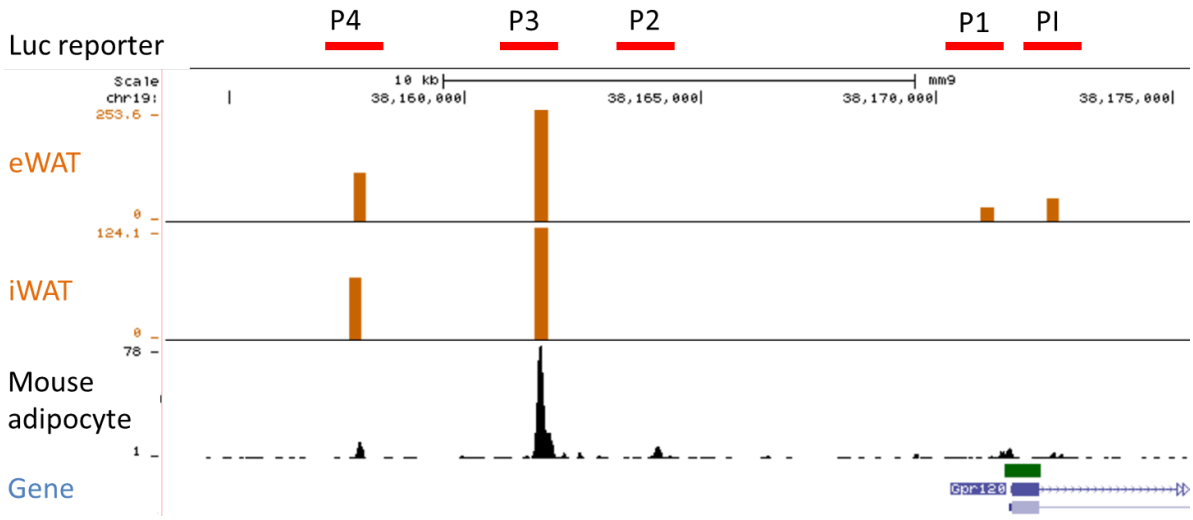

Figure 9: Scheme adapted from UCSC genome browser (http://genome.ucsc.edu). The peaks represent putative PPARγ binding sites obtained from [30,31]. The regions used for luciferase reporter assays are marked with red bars. P 1-4 … peak 1-4, PI … peak intron 1.

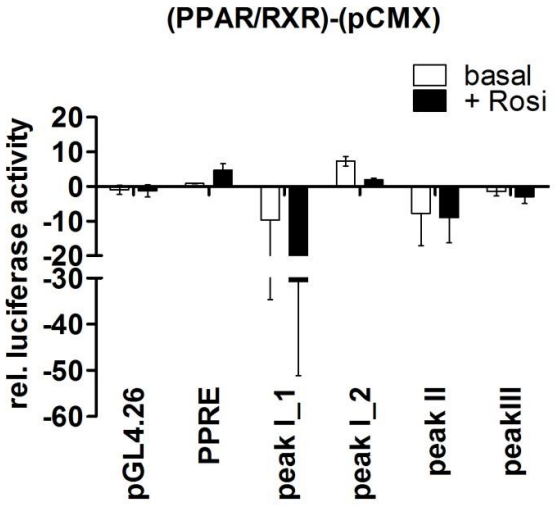

Figure 10: Luciferase activity of PPRE 3x-TK-Luc, and peak I_1+2, II and III in gGL4.26. The values of RXRα/PPARγ contransfected samples are normalized to pCMX as an empty vector and rosiglitazone (10µM for 24 hours) was used to stimulate PPARγ activity. The results of two independent experiments are combined and shown.

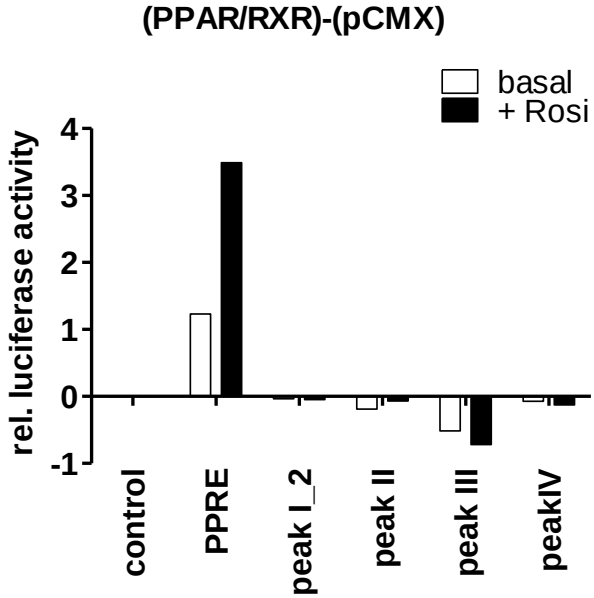

Figure 11: Luciferase activity of PPRE 3x-TK-Luc, peak I_2, II, III and IV in pTK-Luc. The values of RXRα/PPARγ contransfected samples are normalized to pCMX as an empty vector and rosiglitazone (10µM for 24 hours) was used to stimulate PPARγ activity. The result of one representative experiments is shown.

4.3. Expression of GPR120 in different tissues upon the influence of different diets

The tissue expression of GPR120 in different tissues is already known[25], but nothing is known about how the expression changes when mice are fed a diet rich in omega-3 fatty acids such as a fish oil diet (FOD) or a diet which is supplemented with a new synthetic GPR120 agonist, namely L373. Therefore, we aimed to investigate the expression of GPR120 upon feeding the mice these different diets. Brown adipose tissue (BAT) has a relatively high endogenous expression of GPR120 (unpublished data) and there is no big change in expression upon feeding different diets (figure 12). In contrast to that, the expression of GPR120 highly increases in tissues that normally do not have such a high GPR120 expression, such as skeletal muscle (SM) and liver[25]. The diet supplemented with L373 has an especially high impact on the expression of GPR120 in skeletal muscle (figure 12).

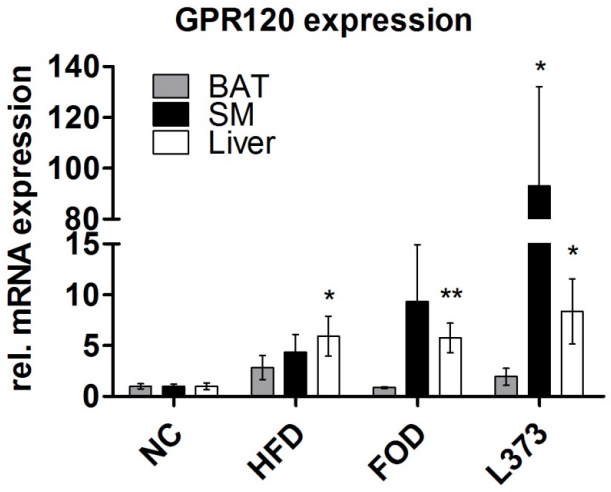

Figure 12: mRNA expression of GPR120 in different tissues upon different diets. C57BL/6 mice were kept on normal chow (NC) or high fat diet (HFD) for 20 weeks from the age of 8 weeks. The mice were changed to fish oil diet (FOD) or diet supplemented with synthetic GPR120 agonist L373 after 15 weeks of HFD and were kept on these diets for further 5 weeks. BAT… brown adipose tissue, SM… skeletal muscle. * p≤0.05, **p≤0.01 compared to NC.

4.4. Expression of GPR120 and other marker genes in microglia from mice on different diets

It was shown by Cintra *et al*. that GPR120 is expressed in the hypothalamus[36], but whether it is expressed in microglia was not assessed. Furthermore, we wanted to investigate if the expression changes upon diet induced obesity. Interestingly, the expression of GPR120 significantly decreases in mice on HFD, whereas a marker for macrophages, F4/80, and inflammatory markers such as interleukin-1β (Il-1β) or tumor necrosis factor α (TNFα) did not change on mRNA level (figure 13).

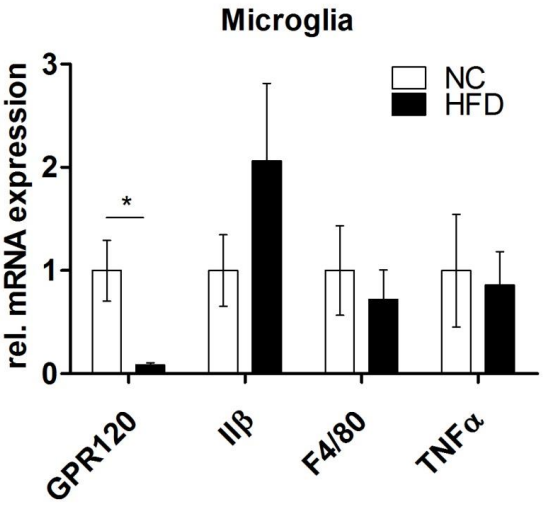

Figure 13: mRNA expression of GPR120 and macrophage/inflammatory marker genes in microglia of mice fed a normal chow diet (NC) or high fat diet (HFD). * p≤0.05

5. Discussion

This work is separated into different parts, but together they address the question how obesity influences the development of inflammation and the progression of insulin resistance. The first part aims to deeper understand the inflammatory processes in the liver when an animal gets obese. As already mentioned in the introduction, these processes are highly complex and the exact role of activated resident Kupffer cells and new macrophages, that get recruited in states of obesity are poorly understood.

The work shown in the first part of this report has been part of a publication which manuscript is under preparation for publication. Together with Dr. Rafael Mayoral, a coauthor of this paper, we improved an existing method to distinguish between resident liver KCs and recruited macrophages. The largest number of cells in the liver is represented by liver hepatocytes which are also the biggest cells in these tissues. For a proper sorting and analysis it was very important to reduce the number of hepatocytes in the cell suspension, what we managed to do with sequential centrifugation steps at a very low speed and the use of a density gradient. Additionally, we faced the problem that the number of KCs was very low and the viability of the cells in culture was not very high. This was especially true for KCs of chow mice, as the number of KCs correlates with the size of the liver, which is much bigger in mice on a long term HFD. To get a higher number of KCs, we increased the number of mice used for the project to 8 per diet. Because many cells died in the overnight culture, the quality of the obtained RNA was also very weak. To overcome this problem, we harvested the cells already after cell sorting by centrifugation and isolated the RNA of these cells directly for downstream analysis.

Until now, it was thought that liver inflammation in states of obesity is mainly caused through the activation of resident KCs[11]. There were already indications that also recruited monocytes may contribute to liver inflammation in this condition[16], but through the help of this work it could be shown, that there is definitely a population of recruited immune cells that do not exist in the liver of healthy mice. It also shows that there is a very heterogeneous pool of immune cells present in the liver. With the help of this technique to distinguish these populations, the role of KCs and RHMs can be studied in more detail.

The second part of this work was the identification and verification of PPARγ binding sites in the promoter region of GPR120. To test this, I generated vectors that contained promoter sequences of GPR120 upstream of an luciferase reporter gene. A binding of PPARγ would

lead to an increase in luciferase activity. Although no increased luciferase activity could be observed with all tested constructs, we are still convinced that PPARγ regulates GPR120 expression under certain circumstances. The assay itself worked well, as the positive construct, containing PPAR response elements showed an increase of luciferase activity upon co-expression with PPARγ and RXRα and a further increase upon rosiglitazone stimulation. It cannot be ruled out, that other cofactors than RXRα, which are not sufficiently expressed in our tested cell lines, are necessary to activate GPR120 expression. Additionally, it is possible that GPR120 is regulated from a PPAR binding site far from its transcription start site. The ongoing work is addressing these possibilities, although it may be difficult to test a distant PPARγ regulation. Additionally, changing the cell system could also improve the performance of the assay. In this work, Cos7 cell and human embryonic kidney (HEK cells) have been tested. Finally, also the used plasmid has influence on the outcome of the assay. We used 2 different plasmids. The first one contained a minimal promoter downstream from the inserted response element and exhibits therefore a stable expression of the luc-gene. Unfortunately, we had very high basal luciferase activities and doubted that changes are detectable. We therefore changed to another vector that we also used as a positive construct (PPRE 3X-TK-Luc), excised the PPRE sequences and inserted our construct. Also this approach did not lead to the expected outcome. This is maybe due to the missing promoter elements that disturbed the assay in the first case. Current investigations are also dealing with this problem.

The last part dealt with the investigation of the expression profile of GPR120 in different tissues under the influence of different diets. The major components of FOD are ω-3 FA such as DHA and eicosapentaenoic acid (C20:5n3, EPA). Numerous studies deal with the investigation of the beneficial properties of long-chain polyunsaturated fatty acids (PUFAs) in the treatment of obesity and its related morbidities such as T2D and cardiovascular diseases[43]. DHA and EPA belong to this group of PUFAs. Oh et al.[22] showed that these fatty acids are ligands for the G-protein coupled receptor GPR120 and that an activation of this receptor decreases inflammation in inflammatory macrophages. Here, we wanted to investigate whether the supplementation of PUFAs in the diet can influence the expression levels of GPR120. Additionally to the FOD, we used a diet supplemented with a synthetic agonist of GPR120 (manuscript submitted). With both diets, we see an upregulation of GPR120 expression in the liver and the skeletal muscle, but also HFD increased the expression, but to a lower extent. There is a very low GPR120 expression on chow diet in these tissues and obviously a high content of ligands for this receptor leads to increased expression. The impact of ω-3 FA and the synthetic GPR120 agonist on the metabolism and

inflammatory pathways in tissues like skeletal muscle and liver can be now studied in more detail.

As already described in the introduction obesity leads to an increased inflammatory state in the whole body, including the brain. To investigate whether GPR120 is expressed in brain macrophages and whether their expression profile is changed upon diet induced obesity, we isolated microglia from mice fed a HFD for 20 weeks. In this experiment we used a column with magnetic beads which are coated with a specific antibody against CD11b. This is a surface marker present on macrophages, including microglia. Using this protocol, only cells that express CD11b should bind to the beads and that is how you elute only microglia from the column in the end. We faced the problem that the high concentration of myelin disturbed the preparation process. Myelin is a highly abundant material in the brain, which is usually found around neurons and axons to insulate these cells. The concentration of myelin is very low in newborns, but highly increases in adult brains[44]. We used brains from adult mice for this study. To improve the microglia preparation method, it would probably be an advantage to use a kit to reduce the amount of myelin prior to the microglia isolation.
Nevertheless, we could isolate a sufficient amount of microglia and investigate the expression of GPR120 in these cells. Interestingly, GPR120 mRNA expression is blunted in mice on HFD, but no changes is the expression of F4/80, a marker for macrophages and the proinflammatory cytokines IL1b and TNFα, that are produced by activated macrophages[45], could be observed. If the decreased GPR120 expression contributes to the increased inflammation in the brain upon HFD is not known and is now a matter of further investigation.

6. Acknowledgements

This work would not have been possible without the support of the Austrian science fund FWF (DK-MCD W01226 and P24143) and the Marshall Plan Scholarship.
I greatly thank Dr. Da Young Oh for her supervision and Dr. Jerrold Olefsky for providing me the opportunity to come to his lab and work in this great environment.

7. Literature

1. Friedman, J. M. Obesity in the new millennium. *Nature* **404,** 632–634 (2000).
2. Osborn, O. & Olefsky, J. M. The cellular and signaling networks linking the immune system and metabolism in disease. *Nat. Med.* **18,** 363–374 (2012).
3. Romacho, T., Elsen, M., Röhrborn, D. & Eckel, J. Adipose Tissue and its Role in Organ Crosstalk. *Acta Physiol. Oxf. Engl.* (2014). doi:10.1111/apha.12246
4. Grunfeld, C. & Feingold, K. R. The metabolic effects of tumor necrosis factor and other cytokines. *Biotherapy* **3,** 143–158 (1991).
5. Hotamisligil, G. S., Shargill, N. S. & Spiegelman, B. M. Adipose expression of tumor necrosis factor-alpha: direct role in obesity-linked insulin resistance. *Science* **259,** 87–91 (1993).
6. Xu, H. *et al.* Chronic inflammation in fat plays a crucial role in the development of obesity-related insulin resistance. *J. Clin. Invest.* **112,** 1821–1830 (2003).
7. Weisberg, S. P. *et al.* Obesity is associated with macrophage accumulation in adipose tissue. *J. Clin. Invest.* **112,** 1796–1808 (2003).
8. Christiansen, T., Richelsen, B. & Bruun, J. M. Monocyte chemoattractant protein-1 is produced in isolated adipocytes, associated with adiposity and reduced after weight loss in morbid obese subjects. *Int. J. Obes. 2005* **29,** 146–150 (2005).
9. Chakrabarti, S. K. *et al.* Evidence for activation of inflammatory lipoxygenase pathways in visceral adipose tissue of obese Zucker rats. *Am. J. Physiol. Endocrinol. Metab.* **300,** E175–187 (2011).
10. Olefsky, J. M. & Glass, C. K. Macrophages, inflammation, and insulin resistance. *Annu. Rev. Physiol.* **72,** 219–246 (2010).
11. Cai, D. *et al.* Local and systemic insulin resistance resulting from hepatic activation of IKK-beta and NF-kappaB. *Nat. Med.* **11,** 183–190 (2005).
12. Gribble, F. M. Metabolism: a higher power for insulin. *Nature* **434,** 965–966 (2005).
13. Seppälä-Lindroos, A. *et al.* Fat accumulation in the liver is associated with defects in insulin suppression of glucose production and serum free fatty acids independent of obesity in normal men. *J. Clin. Endocrinol. Metab.* **87,** 3023–3028 (2002).
14. Angulo, P. Nonalcoholic Fatty Liver Disease. *N. Engl. J. Med.* **346,** 1221–1231 (2002).
15. Wisse, E. Kupffer cell reactions in rat liver under various conditions as observed in the electron microscope. *J. Ultrastruct. Res.* **46,** 499–520 (1974).

16. Obstfeld, A. E. *et al.* C-C chemokine receptor 2 (CCR2) regulates the hepatic recruitment of myeloid cells that promote obesity-induced hepatic steatosis. *Diabetes* **59,** 916–925 (2010).
17. Oh, D. Y., Morinaga, H., Talukdar, S., Bae, E. J. & Olefsky, J. M. Increased macrophage migration into adipose tissue in obese mice. *Diabetes* **61,** 346–354 (2012).
18. Kinoshita, M. *et al.* Characterization of two F4/80-positive Kupffer cell subsets by their function and phenotype in mice. *J. Hepatol.* **53,** 903–910 (2010).
19. Lagerström, M. C. & Schiöth, H. B. Structural diversity of G protein-coupled receptors and significance for drug discovery. *Nat. Rev. Drug Discov.* **7,** 339–357 (2008).
20. Ritter, S. L. & Hall, R. A. Fine-tuning of GPCR activity by receptor-interacting proteins. *Nat. Rev. Mol. Cell Biol.* **10,** 819–830 (2009).
21. Hirasawa, A. *et al.* Free fatty acids regulate gut incretin glucagon-like peptide-1 secretion through GPR120. *Nat. Med.* **11,** 90–94 (2005).
22. Oh, D. Y. *et al.* GPR120 is an omega-3 fatty acid receptor mediating potent anti-inflammatory and insulin-sensitizing effects. *Cell* **142,** 687–698 (2010).
23. Kang, D. S., Tian, X. & Benovic, J. L. Role of β-arrestins and arrestin domain-containing proteins in G protein-coupled receptor trafficking. *Curr. Opin. Cell Biol.* **27C,** 63–71 (2014).
24. Luttrell, L. M. & Lefkowitz, R. J. The role of beta-arrestins in the termination and transduction of G-protein-coupled receptor signals. *J. Cell Sci.* **115,** 455–465 (2002).
25. Gotoh, C. *et al.* The regulation of adipogenesis through GPR120. *Biochem. Biophys. Res. Commun.* **354,** 591–597 (2007).
26. Ichimura, A. *et al.* Dysfunction of lipid sensor GPR120 leads to obesity in both mouse and human. *Nature* **483,** 350–354 (2012).
27. Rosen, E. D. *et al.* PPARγ Is Required for the Differentiation of Adipose Tissue In Vivo and In Vitro. *Mol. Cell* **4,** 611–617 (1999).
28. Bogner-Strauss, J. G. *et al.* Reconstruction of gene association network reveals a transmembrane protein required for adipogenesis and targeted by PPARgamma. *Cell. Mol. Life Sci. CMLS* (2010). doi:10.1007/s00018-010-0424-5
29. Walenta, E. *et al.* α/β-hydrolase domain containing protein 15 (ABHD15)--an adipogenic protein protecting from apoptosis. *PloS One* **8,** e79134 (2013).
30. Siersbæk, M. S. *et al.* Genome-wide profiling of peroxisome proliferator-activated receptor γ in primary epididymal, inguinal, and brown adipocytes reveals depot-selective binding correlated with gene expression. *Mol. Cell. Biol.* **32,** 3452–3463 (2012).
31. Nielsen, R. *et al.* Genome-wide profiling of PPARgamma:RXR and RNA polymerase II occupancy reveals temporal activation of distinct metabolic pathways and changes in RXR dimer composition during adipogenesis. *Genes Dev.* **22,** 2953–2967 (2008).

32. Lefterova, M. I. *et al.* Cell-specific determinants of peroxisome proliferator-activated receptor gamma function in adipocytes and macrophages. *Mol. Cell. Biol.* **30,** 2078–2089 (2010).
33. De Souza, C. T. *et al.* Consumption of a fat-rich diet activates a proinflammatory response and induces insulin resistance in the hypothalamus. *Endocrinology* **146,** 4192–4199 (2005).
34. Kettenmann, H., Hanisch, U.-K., Noda, M. & Verkhratsky, A. Physiology of microglia. *Physiol. Rev.* **91,** 461–553 (2011).
35. Chang, C.-Y. *et al.* Docosahexaenoic acid reduces cellular inflammatory response following permanent focal cerebral ischemia in rats. *J. Nutr. Biochem.* **24,** 2127–2137 (2013).
36. Cintra, D. E. *et al.* Unsaturated Fatty Acids Revert Diet-Induced Hypothalamic Inflammation in Obesity. *PLoS ONE* **7,** e30571 (2012).
37. Hara, T., Hirasawa, A., Ichimura, A., Kimura, I. & Tsujimoto, G. Free fatty acid receptors FFAR1 and GPR120 as novel therapeutic targets for metabolic disorders. *J. Pharm. Sci.* **100,** 3594–3601 (2011).
38. Yoshizaki, T. *et al.* SIRT1 exerts anti-inflammatory effects and improves insulin sensitivity in adipocytes. *Mol. Cell. Biol.* **29,** 1363–1374 (2009).
39. Cardona, A. E., Huang, D., Sasse, M. E. & Ransohoff, R. M. Isolation of murine microglial cells for RNA analysis or flow cytometry. *Nat. Protoc.* **1,** 1947–1951 (2006).
40. Ikarashi, M. *et al.* Distinct development and functions of resident and recruited liver Kupffer cells/macrophages. *J. Leukoc. Biol.* jlb.0313144 (2013). doi:10.1189/jlb.0313144
41. Kim, J. B., Wright, H. M., Wright, M. & Spiegelman, B. M. ADD1/SREBP1 activates PPARgamma through the production of endogenous ligand. *Proc. Natl. Acad. Sci. U. S. A.* **95,** 4333–4337 (1998).
42. Forman, B. M. *et al.* 15-Deoxy-Δ12,14-Prostaglandin J2 is a ligand for the adipocyte determination factor PPARγ. *Cell* **83,** 803–812 (1995).
43. Lorente-Cebrián, S. *et al.* Role of omega-3 fatty acids in obesity, metabolic syndrome, and cardiovascular diseases: a review of the evidence. *J. Physiol. Biochem.* **69,** 633–651 (2013).
44. Poduslo, S. E. & Jang, Y. Myelin development in infant brain. *Neurochem. Res.* **9,** 1615–1626 (1984).
45. Wynn, T. A., Chawla, A. & Pollard, J. W. Macrophage biology in development, homeostasis and disease. *Nature* **496,** 445–455 (2013).

8. Abbreviations

DHA	docosahexaenoic acid
T2D	type 2 diabetes
ATM	adipose tissue macrophage
AT	adipose tissue
KC	Kupffer cell(s)
RHM	recruited hepatic macrophage
WAT	white adipose tissue
GPR120	G-protein coupled receptor 120
HFD	high fat diet
NC	normal chow diet
FOD	fish oil diet
Luc	luciferase
PPAR	peroxisome proliferator-activated receptor
HBSS	Hank's balanced salt solution
TLCK	Na-Tosyl-L-lysine chloromethyl ketone hydrochloride
PBS	Phosphate buffered saline
BSA	Bovine serum albumin
PCR	Polymerase chain reaction
TNF-α	Tumor necrosis factor alpha
Il-1β	interleukin 1 beta
BAT	brown adipose tissue
SM	skeletal muscle
FA	fatty acid
WT	wild type
KO	knock-out
PPRE	PPARγ response element
ω-3	omega-3